Immune evasion by Salmonella: Exploiting the VPAC1/VIP axis in human monocytes

Basim Askar, John Higgins, Paul Barrow and *Neil Foster

School of Veterinary Medicine and Science, University of Nottingham. Nottingham, UK.

*Corresponding author:

Neil Foster

School of Veterinary Medicine and Science

Sutton Bonington campus

University of Nottingham

Nottingham

NG7 2NR

Tel: 0115 9516433

Email: n.foster@nottingham.ac.uk

Running Title: Salmonella exploits host VPAC1

Key Words: Salmonella VIP immune evasion Rab Calmodulin

Abstract

Immune evasion is a critical survival mechanism for bacterial colonization of deeper tissues and may lead to life-threatening conditions such as endotoxemia and sepsis. Understanding these immune evasion pathways would be an important step for the development of novel anti-microbial therapeutics.

Here, we report a hitherto unknown mechanisms by which *Salmonella* exploits an anti-inflammatory pathway in human immune cells to obtain survival advantage. We show that *Salmonella enterica* serovar Typhimurium strain 4/74 significantly (P <0.05) increased expression of mRNA and surface protein of the type 1 receptor (VPAC1) for anti-inflammatory vasoactive intestinal peptide (VIP) in human monocytes.

However, we also show that *S*. Typhimurium induced retrograde recycling of VPAC1 from early endosomes to Rab11a-containing sorting endosomes, associated with the Golgi apparatus, and anterograde trafficking via Rab3a and calmodulin 1. Expression of Rab3a and calmodulin 1 were significantly increased by *S*. Typhimurium infection and W-7 (calmodulin antagonist) decreased VPAC1 expression on the cell membrane while CALP-1 (calmodulin agonist) increased VPAC1 expression (P < 0.05). When infected monocytes were co-cultured with VIP, a significantly higher number of *S*. Typhimurium were recovered from these monocytes, compared to S. Typhimurium recovered from monocytes cultured only in cell media.

We conclude that *S*. Typhimurium infection exploits host VPAC1/VIP to gain survival advantage in human monocytes.

Introduction

Survival of some *Salmonella* serovars in innate immune cells is a critical step for immune evasion and colonization of deeper tissue, which may lead to life-threatening diseases such as Gram negative sepsis or typhoid. Understanding the pathways associated with immune evasion and survival may inform better therapeutic strategies for the treatment of such diseases.

The bi-phasic model for human sepsis proposes a phase of uncontrolled production of inflammatory mediators, which leads to systemic inflammatory response syndrome (SIRS) followed by a compensatory anti-inflammatory response syndrome (CARS) (1-3). The SIRS (acute) phase of sepsis is associated with high systemic concentrations of pro-inflammatory cytokines released by monocytes and macrophages, such as TNF-α, IL-1 and IL-6 (4). Intervention with anti-inflammatories has been proposed as a rational therapeutic avenue during SIRS but specific inhibition of IL-1β or TNF-α has failed (5), while broad ranging anti-inflammatories, such as glucocorticoids, are also widely used in the treatment of sepsis but their effect is debateable, probably due to timing of therapy, dosage and the development of steroid resistance by glucocorticoid receptors (6).

Studies, to date, have indicated that vasoactive intestinal peptide **(**VIP) may have therapeutic potential in the treatment of sepsis. The amino acid structure of VIP is highly conserved throughout the vertebrates and is identical in all mammals apart from guinea pigs (7). In murine models of LPS-induced sepsis, intra-peritoneal administration of low concentrations of VIP (<5 nmol) prevented mortality and this was associated with inhibition of inflammatory cytokines (8). VIP exerts its biological effect via three G-protein coupled receptors; VIP receptor 1 (VPAC1), VPAC2 and a receptor which is also activated via the pituitary adenylate-cyclase activating polypeptide (PAC1). VPAC1 is constitutively expressed by some resting immune cells (9-10) and the immunosuppressive action of VIP on LPS-stimulated murine macrophages occurs via

this receptor (11). Increased VPAC1 expression was also reported in human peripheral blood monocytes following intravenous administration of LPS and correlates with increased VIP concentration in sera (12). However, using virulent *S*. Typhimurium (rather than LPS) we have shown that VIP promotes survival of *S*. Typhimurium within human monocytes, which is associated with inhibition of proinflammatory cytokines and increased survival of the infected cells (13). This may indicate that *S*. Typhimurium increases receptivity of monocytes to VIP, specifically to inhibit production of inflammatory mediators, thus gaining survival advantage. It is known that upon activation, VPAC1 is internalized and may be recycled back to the cell membrane (14-16) but nothing is known about the intracellular pathways utilized to achieve this and nothing has been reported regarding the effect of *Salmonella* infection on VPAC1 or these pathways.

The aim of this current study was to investigate whether *S*. Typhimurium induces VPAC1 expression in human monocytes, and, if so, to determine the intracellular pathways responsible for this.

Material and methods

Reagents

Unless otherwise stated all reagents were purchased from Sigma-Aldrich, Poole, Dorset UK. PCR and microarray reagents were purchased from Qiagen, Manchester, UK.

Bioethics

Human blood used in this study was obtained with patient consent. All studies were conducted following approval by local ethics committees. Studies were performed on 5 separate occasions, therefore blood from 5 individual humans.

Bacterial culture and strains.

S. Typhimurium 4/74 (17) were grown in Luria-Bertani (LB) broth (Life Technologies Ltd., Paisley, United Kingdom) for 18 h at 37°C under agitation. The bacteria were then sub-cultured in fresh LB broth for 4 h to late log phase (established by conventional counts of CFU). Prior to incubation with monocytes, bacteria were adjusted to a multiplicity of infection (MOI) of 10.

Isolation of peripheral blood monocytes (PBM)

Human blood was purchased from the blood transfusion service (Sheffield, UK). The blood was diluted with sterile PBS then gently poured onto Histopaque-1077, prior to isolation of the buffy coat, as standard procedure. After appropriate washing steps, buffy coat supernatants were resuspended with appropriate amounts of cold MACS buffer and anti-CD14 antibody coated micromagnetic beads (Miltenyi Biotech, Bisley, Surrey UK) according to the manufacturer's instructions. The viability of isolated monocytes was assessed using Trypan blue (10% v/v) and was found to be > 90 % prior to use.

***Salmonella* invasion assays**

Monocytes were firstly washed with sterile PBS prior to culture with *S*. Typhimurium 4/74 at a multiplicity of infection (MOI) of 10:1 at 37 ^{0}C and 5% CO_2 for 60 min with or without VIP (10^{-7} M). The cells were then washed and cultured with RPMI media containing 100 μg/ml gentamycin and incubated for a further 60 min. The monocytes were washed and the media was substituted with RPMI containing 25 μg/ml of gentamycin for a further 2, 6 or 24 h post-infection (pi) in total. The cells were then washed three times with PBS at room temperature and then lysed using 1 % Triton X (Fisher Scientific LTD, Loughborough, UK) for 15 minutes at 37 ^{0}C. Intracellular bacterial counts were determined by serial dilution at different time points of 2,

6 and 24h pi. Viable bacterial cell counts were measured as colony forming units per ml (CFU/ml). All counts were performed in triplicate on 5 separate occasions.

PCR analysis

RNA was purified from treated or control monocytes by standard methods, using Rneasy plus kits (Qiagen, Hilden, Germany). RNA quantity and quality were measured using a NanoDrop 8000 spectrophotometer (Thermo Scientific, Warrington, UK) and was converted into complimentary DNA (cDNA) using a SuperScipt first strand DNA synthesis kit (Invitrogen, Carlbad, CA, USA). For quantitative PCR analysis primers and probes were designed using a universal probe library (Roche Diagnostics, Mannheim, Germany). A PCR reaction volume (20 µl) consisting of 10 µl Light Cycler 480 Probes Master (Roche, Germany), 1 µm of each forward and reverse primer (Eurofins MWG, Operon, Germany) and 0.2 µl, labelled with Fluorescein and dark quencher dye. The total volume was adjusted to 20 µl using PCR water. In negative control wells, PCR water was added instead of cDNA. Standard curves of target and reference genes were performed at dilution ranges between 1:10- 10^5. Thermal cycles consisted of denaturing at 95 ^{0}C for 10 min and 40 cycles of sample amplification at 95 ^{0}C for 10 secs, 60 ^{0}C for 30 secs, 72 ^{0}C for 1 min and cooling at 40 ^{0}C for 30 secs, performed using a Roche applied sciences light cycler 480 (Roche, Germany). All data was normalised to unstimulated monocytes, or expression in uninfected mouse tissues for *in vivo* studies, and quantification was determined by comparison to the reference gene using the Pfaffl method (18). All primers and probes used in PCR are shown in Table 1.

Immunofluorescence studies

Freshly isolated monocytes (5 x 10^5) were cultured on glass cover slips (VWR International Ltd, Leighton Buzzard, UK) placed in 24 well culture dishes, for 6h. The monocytes were then

infected with *S*. Typhimurium (6h pi) or cultured with VIP (10^{-7} M) in RPMI media for 6h, or cultured for 6 h in RPMI media without bacteria or VIP (uninfected control). After 6h the monocytes were washed 3 times in PBS and fixed in paraformaldehyde (4% v/v) for 10 min at room temperature prior to permeabilization in Triton-X (Fisher Scientific, Loughborough, UK) (0.2% v/v) for 10 min. After washing 3 times in PBS, the monocytes were incubated at room temperature for 30 min in blocking buffer; bovine serum albumin (BSA) solution (3% w/v in PBS). After washing 3 times in PBS the monocytes were incubated for 60 min with appropriate primary antibody (300 µl), washed 3 times in PBS and incubated with secondary antibody (300 µl) in the dark for 45 min on an end-to-end shaker. After a final washing step, the coverslips were placed onto microscope slides prior to adding Vectashield hard set mounting medium. All slides were examined using a TCS SP2 confocal microscope (Leica Micosystems, Heidelburg, Germany). Each panel shown in figures 3 and 4 are merged plane image captures 4 µm below the cell surface. To prevent spectral overlap, Alexa 488 and Alexa 647 fluorophore conjugates were chosen and bypass filtering was applied to prevent bleed through. Laser intensity and detector gain were optimised and standardised throughout. Each experiment was repeated in triplicate on 5 separate occasions. All primary and secondary antibodies used during the confocal analysis, together with suppliers are shown in Table 2.

Flow cytometry

S. Typhimurium infected monocytes (6h pi), monocytes cultured with VIP and monocytes cultured only in RPMI media (unstimulated controls) for 6h were centrifuged at 300 x g for 10 min. The supernatant was discarded and the cell pellet was washed 3 times by resuspension in PBS and centrifugation at 300 x g for 10 min, repeated a further 2 times. Monocytes were either left non-permeabilised or permeabilised for 10 min in Triton-X (Fisher Scientific, UK) (0.2%

v/v) and washed a further 3 times prior to incubation at room temperature for 30 min in blocking buffer (PBS and BSA 3% w/v). After washing 3 times in PBS the monocytes were incubated for 60 min with mouse anti-human VPAC1 IgG2a (300 µl), washed 3 times in PBS and incubated with rat anti-mouse IgG2a-Alexa-488 (300 µl) (Table 2) in the dark for 45 min on an end-to-end shaker. The monocytes were then washed 3 times prior to analysing antibody fluorescence using a FACScan flow cytometer (Becton Dickinson, NJ, USA). Gating of the cell populations were performed, according to journal guidelines, using CD14 expression (92% of the population) and side scatter (SSC). In FACS plots, quadrants were set according to fluorescence expressed by monocytes incubated only with secondary antibody (control) (lower left quadrant) and fluorescence in test cell populations were compared to these. Data analysis was performed using FACSDiva software (Becton Dickinson, USA). Each experiment was performed in triplicate on 5 separate occasions.

Calmodulin 1 (CAM1) agonist and antagonist studies

To investigate the effect of CAM1 on VPAC1 expression, freshly isolated monocytes (5×10^5) were incubated for 2h with either the CAM1 agonist; calcium-like peptide 1 (CALP1) (20 µM) (Tocris Bioscience, Abingdon, UK) or the CAM1 antagonist; W-7 (30 µM) (Sigma-Aldrich, Poole, UK). The concentrations of agonist and antagonist chosen in these experiments were determined via dose response and output curves (data not shown). PCR and flow cytometry were then performed to assess VPAC1 expression in *S*. Typhimurium infected and uninfected monocytes, as stated above at 6h pi. Mean data was obtained from experiments performed in triplicate on 5 separate occasions.

Statistical Analysis

Two-tailed unpaired student's *t* test or one-way ANOVA were performed to determine significant differences between different groups (control negative, *S.* Typhimurium infected, with or without VIP) using Graph Pad Prism software. Bonferroni's multiple comparisons test was applied to examine significant difference between the means of more than two groups, following ANOVA. Significance values were determined at the 95% confidence limit ($P < 0.05$).

Results

S. Typhimurium increases VPAC1 expression

High constitutive expression of VPAC1 was detected by RTPCR but following S. Typhimurium infection, expression of VPAC1 increased further (Fig 1A). *S.* Typhimurium significantly increased VPAC1 mRNA expression by around 5 fold above expression in resting monocytes ($P < 0.05$) but VPAC1 expression was not differentially expressed when monocytes were cultured with VIP (Fig 1B). After 6 and 24h pi, significantly more *S.* Typhimurium were recovered from infected monocytes which had been co-cultured with VIP, compared to infected monocytes without VIP ($P < 0.05$) (Fig 1C).

Following FACS analyses, we also detected a 50% increase in the immunoreactivity of VPAC1 protein in the cytosol of monocytes after 6h pi with *S.* Typhimurium, which was highly significant ($P < 0.01$) when compared to VPAC1 protein in the cytosol of monocytes incubated with VIP or uninfected monocytes (Fig 2A and C). FACS analysis also showed thatVPAC1 protein was increased on the surface of monocytes infected with *S.* Typhimurium by around 30% and this increase was also significant ($P < 0.05$) when compared to VPAC1 protein in the cytosol of monocytes incubated with VIP or uninfected monocytes (Fig 2B and D).

Retrograde recycling of VPAC1 occurs following *S*. Typhimurium infection of monocytes

Confocal microscopy showed that VPAC1 expression was similar in monocytes incubated with VIP to that in unstimulated monocytes (Fig 3A), this was low and was partially co-localized with the early endosome antigen 1 (EEA1) within the early/sorting endosome (SE). However, VPAC1 immunofluorescent intensity was greatly increased and was strongly co-localized with EEA1 following *S*. Typhimurium infection (Fig 3A). Following internalization of VPAC1 in the SE of *S*. typhimurium-infected monocytes, VPAC1 was trafficked from the SE to recycling endosomes (REs) associated with the TGN (retrograde trafficking). This was indicated by strong co-localization of VPAC1 with Rab11a (Fig 3B) and concomitant co-localisation of Rab11a with the trans-Golgi network (TGN), using TGN protein 46 (TGN46) as a marker Fig 3C).

***S*. Typhimurium induces anterograde recycling of VPAC1 via Rab3a/CAM1.**

Further trafficking of VPAC1 in monocyte exosomes, following *S*. Typhimurium Infection, was indicated by strong co-localisation of VPAC1 with the membrane docking protein Rab3a (Fig 4A) which was concomitantly co-localised with CAM1 (Fig 4B). Subsequent qPCR analysis showed that *S*. Typhimurium infection induced a >5 fold ($P < 0.05$) increase in both Rab3A and CAM1 above that measured in unstimulated monocytes or monocytes cultured with VIP (Fig 4C). Addition of a CAM1 agonist (CALP1) to cell cultures significantly increased VPAC1 mRNA expression in *S*. Typhimurium-infected monocytes ($P <0.05$), whereas addition of a CAM1 antagonist (W-7) significantly decreased VPAC1 mRNA expression ($P <0.05$) (Fig 4D). FACS analyses also indicated a causal association between CAM1 and VPAC1 protein expression. These showed that expression of VPAC1 protein on the surface of *S*. Typhimurium-infected monocytes was increased by CALP1 and decreased by W-7 (Fig 5G-I) compared to uninfected monocytes (Fig 5A-C) or monocytes cultured with VIP (Fig 5D-F) and in both cases

these changes were significant (P <0.05). P- values were calculated by ANOVA analysis of mean expression detected for each experimental group (Shown in Fig 5K). A diagrammatic model of intracellular cycling of VPAC1, induced by *S*. Typhimurium infection, is shown in Fig 5L.

Discussion

We show that *S*. Typhimurium increased expression of VPAC1 in human monocytes and this was associated with increased intracellular survival of the bacteria, when infected monocytes were co-cultured with VIP. This is in accordance with a study by Storka et al., (2013) (12) who reported a >30% increase in VPAC1 expression in monocytes isolated from human volunteers 24h after infusion of lipopolysaccharide (LPS) from *Escherichia coli* and this was correlated with an increased concentration of VIP in plasma. However, at least some of this effect is probably due to increased monocyte survival (13, 19) but the effect is not merely due to LPS, which we found to induce lower levels of VPAC1 by both qPCR and FACS analyses compared to *Salmonella* infection (data not shown).

Murine studies have indicated that the immunosuppressive effect of VIP occurs uniquely via VPAC1 (11) and that VIP/VPAC1 interaction regulates production of inflammatory mediators associated with mortality in sepsis (8), which may have evolved to protect the host. However, studies using viable *Salmonella,* rather than LPS have shown that VIP down-regulates inflammatory mediators and increases *Salmonella* survival in human monocytes (13, 19) and murine macrophages (20). We therefore hypothesised that *S*. Typhimurium actively utilises the VPAC1/VIP axis for its own survival advantage.

We now show that *S.* Typhimurium not only increased VPAC1 mRNA and protein expression but also induced VPAC1 recycling to the cell membrane. The initial step in this process was internalization of VPAC1 into EEA-1-containing SE. EEA-1 is required for tethering, docking and fusion of the SE to Soluble NSF Attachment Protein Receptor (SNARE), which subsequently leads to endosomal shipment (21). A previous study has shown that internalisation and localisation of VPAC1 in the SE occurred in VPAC1 transinfected CHO cells, following culture with VIP (22). However, in this latter study, VPAC1 was not recycled back to the cell membrane and in accordance with this, we show that VIP did not increase VPAC1 expression on the cell membrane.

Internalised proteins may be trafficked via the SE to late endosomes and lysosomes (which may prevent further recycling) or to the trans-Golgi network (TGN) (retrograde transport) which may sort the proteins into recycling endosomes (REs) for subsequent transport back to the cell membrane (anterograde transport) (23-24). This requires interaction with Ras-associated binding (Rab) proteins, which are small GTPases involved in intracellular trafficking of protein cargo from the SE to downstream endosomes, including the RE, and the docking of transport vesicles with membrane targets (25). In our study, *S.* Typhimurium-induced retrograde transport of VPAC1 was indicated by strong co-localisation of VPAC1 with Rab11a, one of the best studied markers of REs (26) and TGN protein 46 (TGN46). The TGN is the critical region on the Golgi apparatus, which collects and sorts newly synthesised proteins and proteins relayed to it from REs (27-28). Some bacterial toxins, such as Shiga toxin, produced by *Shigella dysenteriae* (29), HIV envelope protein (30) and the immunosuppressive HIV nef protein (31-32) are trafficked from the cell surface via retrograde transport. However, our study is the first to show that *S.* Typhimurium (or any other pathogen) induces retrograde transporting of VPAC1.

The results we obtained also suggested that *S*. Typhimurium induced anterograde transport of VPAC1 via CAM1/Rab3a. The importance of Ca2+ in regulated exocytosis has been known for a number of years (33) and a study by MacKenzie et al., (34) also reported a positive correlation between Ca2+ concentration and VPAC1 density. Ca2+ binding by CAM1 forms Ca2+/CAM1 complexes that bind to Rab3a, which subsequently causes switching of Rab3a from a GDP-bound (inactive form) to a GTP-bound (active) form (35). It is possible that the increase in CAM1 and Rab3a mRNA we show may increase calcium binding and active Rab3a and thus VPAC1 binding and transport to the cell membrane. Active Rab3a is a constituent protein in secretory vesicles within PC-12 cells and, in newly formed secretory vesicles associated with the TGN in pancreatic acinar cells (36) and is involved in the docking and exocytosis of secretory vesicles (37). Very little has been reported regarding Rab3a in immune cells but a study by Abu-Amer et al., (1999) (38) has shown that Rab3a expression is increased in murine bone marrow derived macrophages stimulated with LPS, although this was not studied in the context of VPAC1. We also show that *S*. Typhimurium (which contains LPS) significantly increased Rab3a and CAM1 mRNA expression in monocytes. Moreover, our results show a causal link between CAM1 and VPAC1 expression on the monocyte membrane. However, the effect of CAM1 agonist or antagonist was not absolute, thus suggesting that other factors (possibly Rab3a itself) also directly affect VPAC1 expression on the monocyte surface.

Only a fraction of newly synthesised VPAC1 become inserted into cell membranes, due to conformational misfolding (16) and although *S*. Typhimurium infection increased VPAC1 mRNA expression, it is possible that *S*. Typhimurium-induced recycling of VPAC1 via retrograde/anterograde pathways overcomes low surface expression due to misfolding. This

would facilitate greater interaction with the increased concentration of VIP in serum, as shown by Storka et al., (2013) (12).

In conclusion, *S*. Typhimurium exploits the VPAC1/VIP axis to increase survival in human monocytes, this is achieved, at least in part, by retrograde and anterograde recycling of VPAC1 via CAM1.

Acknowledgments

We would like to thank Mr Scott Hulme for technical support.

Funding support: The work was funded by a University of Duhok / Kurdistan Region of Iraq scholarship awarded to BA.

Conflict of interest

The authors have none to declare.

References

1. Annane D, Bellissant E, Cavaillon JM. Septic shock. *Lancet* 2005; **365**:63-78.

2. Davis BH. 2005. Improved diagnostic approaches to infection/sepsis detection. *Expert Rev Mol Diagn* 2005; **5**:193-207.

3. Ward NS, Casserly B, Ayala A. The compensatory anti-inflammatory response syndrome (CARS) in critically ill patients. *Clin Chest Med* 2008; **29**:617-625.

4. Danikas DD, Karakantza M, Theodorou GL, Sakellaropoulos GC, Gogos CA. Prognostic value of phagocytic activity of neutrophils and monocytes in sepsis. Correlation to CD64 and CD14 antigen expression. *Clin Exp Immunol* 2008; **154**:87-97.

5. Cohen J. Sepsis and septic shock: inching forwards. *Clin Med* 2009; **9**:256-257.

6. Antonucci E, Fiaccadori E, Taccone FS, Vincent JL. Glucocorticoid administration in sepsis and septic shock: time for a paradigm change? *Minerva Anestesiol* 2014; **80**:1058-1062.

7. Du BH, Eng J, Hulmes JD, Chang M, Pan YC, Yalow RS. Guinea pig has a unique mammalian VIP. *Biochem Biophys Res Commun* 1985; **128**:1093-1098.

8. Delgado M, Martinez C, Pozo D, Calvo JR, Leceta J, Ganea D, Gomariz RP. Vasoactive intestinal peptide (VIP) and pituitary adenylate cyclase-activation polypeptide (PACAP) protect mice from lethal endotoxemia through the inhibition of TNF-α and IL-6. *J. Immunol* 1999; **162**:1200-1205.

9. Lara-Marquez M, O'Doriso M, O'Doriso T, Shah M, Karacay B. Selective gene expression and activation-dependent regulation of vasoactive intestinal peptide receptor type 1 and type 2 in human T cells. *J. Immunol* 2001; **166**:2522-2530.

10. EL Zein, N, Corazza F, Sariban E. The neuropeptide pituitary adenylate cyclase activating protein is a physiological activator of human monocytes. *Cell Signal* 2006; **182**:162-173.

11. Delgado M, Marie JC, Martinez C, Abad C, Leceta J. Anti-inflammatory properties of the type 1 and type 2 vasoactive intestinal peptide receptors: role in lethal endotoxic shock. *Eur J. Immunol* 2000; **30**:3236-3246.

12. Storka A, Burian B, Führlinger G, Clive T, Crevenna R, Gsur A, Mosgöller W, Wolzt M. VPAC1 receptor expression in peripheral blood mononuclear cells in a human endotoxemia model. *J. Transl Med* 2013; **11**:117.

13. Askar B, Ibrahim H, Barrow PA, Foster N. Vasoactive intestinal peptide (VIP) differentially affects inflammatory immune responses in human monocytes infected with viable Salmonella or stimulated with LPS. *Peptides* 2015; **71**:188-195.

14. Boissard C, Marie JC, Hejblum G, Gespach C, Rosselin G. Vasoactive intestinal peptide receptor regulation and reversible desensitization in human colonic carcinoma cells in culture. *Cancer Res* 1986; **46**:4406–4413.

15. Nachtergael I, Gaspard N, Langlet C, Robberecht P, Langer I. Asn229 in the third helix of VPAC1 receptor is essential for receptor activation but not for receptor phosphorylation and internalization: comparison with Asn216 in VPAC2 receptor. *Cell Signal* 2006; **12**:2121-2130.

16. Langer I, Leroy K, Gaspard N, Brion JP, Robberecht P. Cell surface targeting of VPAC1 receptors: evidence for implication of a quality control system and the proteasome. *Biochim Biophys Act* 2008; **1783**:1663-16672.

17. Rankin JD, Taylor RJ. The estimation of doses of *Salmonella typhimurium* suitable for the experimental production of diseases in calves. *Vet Rec* 1966; **78**: 706-707.

18. Pfaffl MW. A new mathematical model for relative quantification in real time RT-PCR. *Nucleic acids Res* 2001; **29**:e45.

19. Ibrahim H, Askar B, Barrow PA, Foster N. Dysregulation of JAK/STAT genes by vasoactive intestinal peptide (VIP) in Salmonella-infected monocytes may inhibit its therapeutic potential in human sepsis. *Cytokine* 2018; **105**:49-56.

20. Foster N, Hulme SD, Barrow PA. Vasoactive intestinal peptide (VIP) prevents killing of virulent and phoP mutant Salmonella typhimurium by inhibiting IFN-gamma stimulated NADPH oxidative pathways in murine macrophages. *Cytokine* 2006; **36**:134-140.

21. Christoforidis S, McBride HM, Burgoyne RD, Zerial M. The Rab5 effector EEA1 is a core component of endosome docking. *Nature* 1999; **397**: 621-625.

22. Langer I, Gaspard N, Robberecht P. Pharmacological properties of Chinese hamster ovary cells coexpressing two vasoactive intestinal peptide receptors (hVPAC1 and hVPAC2). *Br J Pharmacol* 2006; **148**:1051-1059.

23. Bonafacino JS, Rojas R. Retrograde transport from endosomes to the trans-Golgi network. *Nat Rev Mol Cell Biol* 2006; **7**:568-579.

24. Hsu VW, Prekeris R. Transport at the recycling endosome. 2010. *Curr Opin Cell Biol* 2010; **22**:528-534.

25. Bhuin T, Roy JK. Rab 11 in disease progression. *Int J Mol Cell Med* 2015; **4**:1-8.

26. Van Ijzendoorn SC. Recycling endosomes. *J. Cell Sci* 2006; **119**:1679-1681.

27. Gu F, Crump CM Thomas G. Trans-Golgi network sorting. *Cell Mol Life Sci* 2001; **58**:1067-1084.

28. Guo Y, Sirkis DW, Schekman R. Protein sorting at the trans-Golgi network. *Annu Rev Cell Dev Biol* 2014; **30**:169-206.

29. Lamaze C, Johannes L. Intracellular trafficking of bacterial and plant toxins. Comprehensive sourcebook of bacterial toxins. J.E. Alouf, M.R. Popoff (Eds.) (Third Edition), Academic Press, London (2006).

30. Lopez-Verges S, Camus G, Blot G, Beauvoir R, Benarous R, Berlioz-Torrent C. Tail-interacting protein TIP47 is a connector between Gag and Env and is required for Env incorporation into HIV-1 virions. *Proc. Natl. Acad. Sci. USA* 2006; **103**:14947-14952.

31. Blagoveshchenskaya AD, Thomas L, Feliciangeli SF, Hung CH, Thomas G. HIV-1 Nef downregulates MHC-I by a PACS-1 and PI3K-regulated ARF6 endocytic pathway. *Cell* 2002; **111**:853-866.

32. Chaudhry A, Das SR, Jameel J, George A, Bal V, Mayor S, Rath S. HIV-1 Nef induces a Rab11-dependent routing of endocytosed immune costimulatory proteins CD80 and CD86 to the Golgi. *Traffic* 2008; **9**:1925-1935.

33. Burgoyne RD, Morgan A. Ca2+and secretory vesicle dynamics. *Trends Neurosci* 1995; **18**:191–196.

34. MacKenzie CJ, Lutz E, McCulloch DA, Mitchell R, Harmar AJ. Phospholipase C Activation by VIP1 and VIP2 Receptors Expressed in COS 7 Cells Involves a Pertussis Toxin-Sensitive Mechanism. *Ann NY Acad Sci USA* 1996; **805**: 579-584.

35. Park J-B, Kim J-S, Kim J-Y, Lee J-Y, Jaebong J-B, Kim J-Y, Seo J-Y, Kim A-R. GTP binds to Rab3A in a complex with Ca2+/calmodulin. *Biochem. J* 2001; **362**:651–657.

36. Jena BP, Gumkowski FD, Konieczko EM, von Mollard GF, Jahn R, Jamieson JD. Redistribution of a rab3-like GTP-binding protein from secretory granules to the Golgi complex in pancreatic acinar cells during regulated exocytosis. *J Cell Biol* 1994; **124**: 43-53.

37. Schlüter OM, Khvotchev M, Jahn R, Südhof TC. Localization versus function of Rab3 proteins. Evidence for a common regulatory role in controlling fusion. *J. Biochem* 2002; **277**:40919-4029.

38. Abu-Amer Y, Teitelbaum SL, Chappel JC, Schlesinger P, Ross FP. Expression and regulation of RAB3 proteins in osteoclasts and their precursors. *J Bone Miner Res* 1999; **14**:1855-1860.

Figure Legends

Table 1. Forward and reverse primers and probes used in PCR reactions.

Forward and reverse primers and probes are shown for each gene analysed by PCR.

Table 2. Primary and secondary antibodies used in confocal microscope analysis and flow cytometry.

The type and concentration of primary and secondary antibodies, together with secondary antibody fluorophore conjugates, together with commercial suppliers, are shown.

Figure 1. Increased survival of *S*. Typhimurium 4/74 in human monocytes co-cultured with VIP is associated with increased expression of VPAC1.

Reverse transcription (rt) PCR showing constitutive and *S*. Typhimurium-induced expression of VPAC1 in monocytes after 6h post-infection (pi.). Comparison between VPAC1 expression is also shown with the reference gene β-actin, which is unchanged in both uninfected and infected monocytes. (B) Quantitative PCR (qPCR) showing expression of VPAC1 after 6h pi in monocytes infected with S. Typhimurium or cultured with VIP (10^{-7} M). Fold changes are

expressed in comparison with mRNA expression measured in unstimulated (control) monocytes, assigned an arbitrary expression value of 1. (C) Recovery of *S*. Typhimurium from monocytes cultured with or without VIP (10^{-7} M) at different times post-infection (pi). White bar = 2h pi, Grey bar = 6h pi, Black bar = 24h pi. Histograms (B and C) show means calculated from 5 separate experiments performed in triplicate. Connecting bars show significant differences at P = 0.05, error bars show standard deviation from the mean.

Figure 2. *S*. Typhimurium 4/74 increases VPAC1 protein in the cytosol and cell membrane of human monocytes.

VPAC1 expression is shown in representative FACS analyses of 5 independent experiments performed in (A) the cytoplasm (permeabilised) and (B) cell membrane (non-permeablised) at 6h pi. In all cases, lower left quadrants were set according to fluorescence expressed by monocytes incubated with secondary antibody only (control). Histograms show mean population sizes expressing VPAC1 after each treatment; permeabilised monocytes (C) and non-permeabilsed monocytes (D) calculated from 5 independent experiments performed in triplicate. Connecting bars show significant differences at P = 0.01-0.05, error bars show standard deviation from the mean.

Figure 3. *S*. Typhimurium infection stimulates retrograde transported of VPAC1 from early/sorting endosome to Rab11a-containing recycling endosome localized with the trans-Golgi network in human monocytes.

Confocal Laser Scanning Microscopy showing co-localization of VPAC1 with EEA1 and Rab11a in human monocytes, each panel shows a merged plane image 4 μm below the cell

surface. (A) Co-localization of VPAC1 immunofluorescence (green Alexa 488) with early endosome antigen 1 (red Alexa 647) (white arrows) with increased levels of VPAC1/EEA1 association in *S.* Typhimurium infected monocytes at 6h pi.

(B) Co-localisation of VPAC1 (green Alexa 488) with Rab11a (red Alexa 647) (white arrows) is shown only in *S.* Typhimurium infected cells and in (C) co-localisation of Rab11a (red Alexa 647) with TGN46 (green Alexa 488) (white arrows) is shown only in *S.* Typhimurium infected cells. CLSM images shown are representative of 5 independent experiments performed in triplicate. Scale bar (bottom left) = 20 μm.

Figure 4. *S.* Typhimurium 4/74 induces packaging of VPAC1 within Rab3a/CAM1 containing secretory vesicles for anterograde transport to the cell membrane of human monocytes.

(A-B) Confocal Laser Scanning Microscopy showing co-localization of VPAC1 with Rab3a and CAM1. Each panel shows a merged plane image 4 μm below the cell surface.

(A) Co-localisation of VPAC1 (green Alexa 488) with Rab3a (red Alexa 647) (white arrows) in *S.* Typhimurium infected monocytes. (B) Co-localisation of CAM1 (green Alexa 488) with Rab3a (red Alexa 647) (white arrows) in *S.* Typhimurium infected monocytes. Images shown are representative of 5 independent experiments performed in triplicate. Scale bar (bottom left) = 20 μm. (C) qPCR showing increased expression of Rab3a and CAM1 mRNA in monocytes 6h pi with *S.* Typhimurium. (D) qPCR showing fold changes in VPAC1 mRNA with or without CAM1 agonist (CALP1) or antagonist (W-7). Each bar is a mean of 5 independent experiments performed in triplicate. White bar = Without agonist/antagonist, Black bar = + CALP1 (agonist), Grey bar = + W-1 (antagonist). Connecting bars show significant differences at P = 0.05, error

bars show standard deviation from the mean. Fold changes are expressed as a comparison with mRNA expression measured in unstimulated (control) monocytes after 6h, assigned an arbitrary expression value of 1.

Figure 5. CAM1 increases VPAC1 protein expression on the cell membrane of monocytes infected with *S*. Typhimurium 4/74.

(A-J) FACS analysis showing VPAC1 expression on the monocyte membrane 6h pi with *S*. Typhimurium or monocytes cultured with VIP (10^{-7} M) for 6h, with or without CAM1 agonist (CALP1; 20μg/ml) or CAM1 antagonist (W-7; 30 μg/ml). FACS analyses shown are representative of experiments performed in triplicate on 5 separate occasions. Y-axes, SSC = Side scatter, X-axis = VPAC1 expression. Quantitative analysis of experimental means are shown in (K). Black bars = 2h post-treatment treatment/infection, White bars = 6h post-treatment/infection and Grey bars = 24h post-treatment/infection. Connecting bars show significant differences at P = 0.05, error bars show standard deviation from the mean.
(L) Diagrammatic representation of *S*. Typhimurium induced trafficking of VPAC1 receptors. (1) *S*. Typhimurium invades monocyte. (2) VPAC1 is packages in the EEA1 positive sorting endosome (SE). (3) Retrograde transport of VPAC1 occurs via Rab11a positive recycling endosome (RE) which is associated with TGN46 on the Golgi apparatus. (4) Anterograde transport of VPAC1 occurs via Rab3a/CAM1 positive secretory vesicle (SV).

499

500

501

502

Fig 1. Askar et al

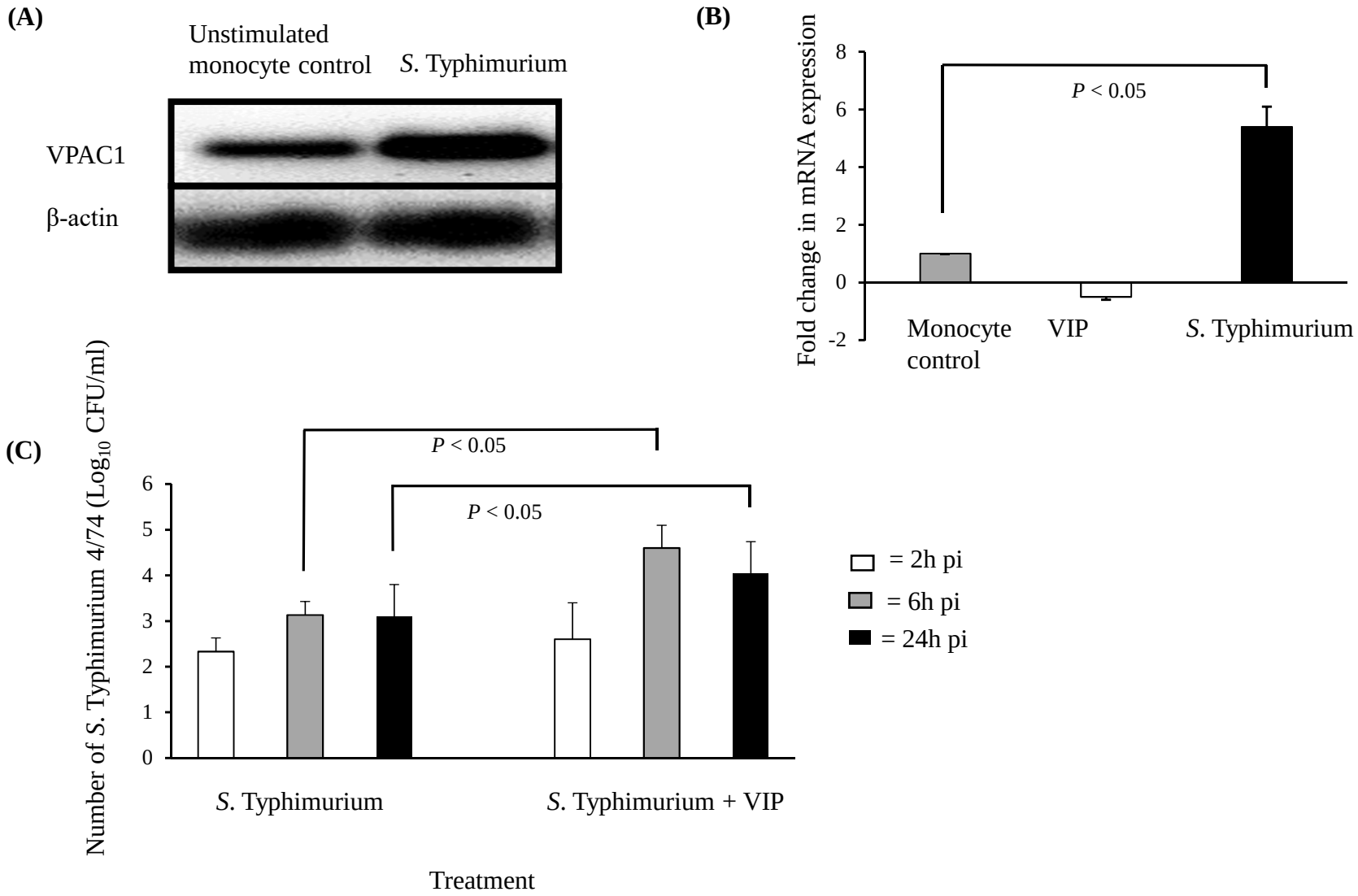


Fig 2. Askar et al

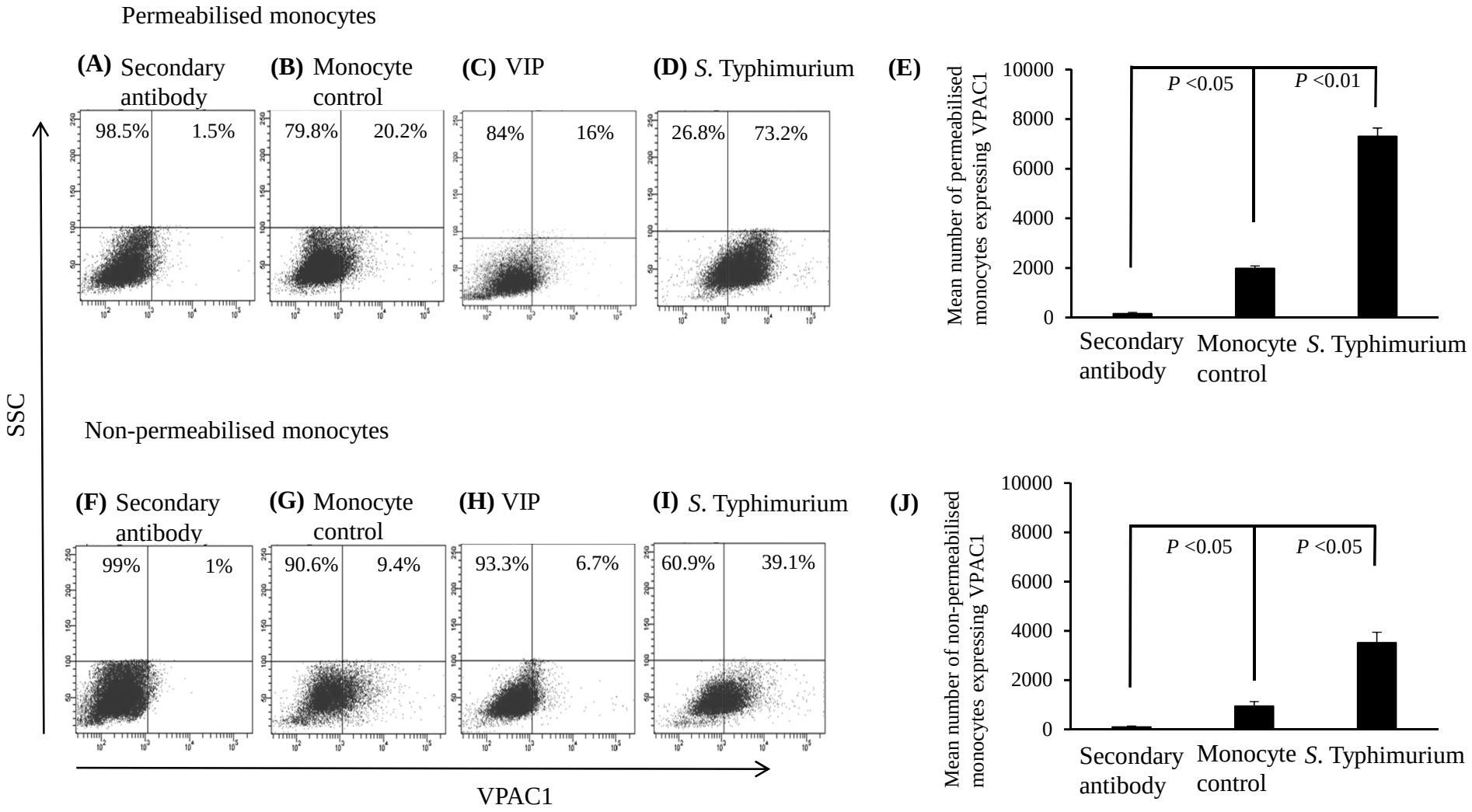


Fig 3. Askar et al

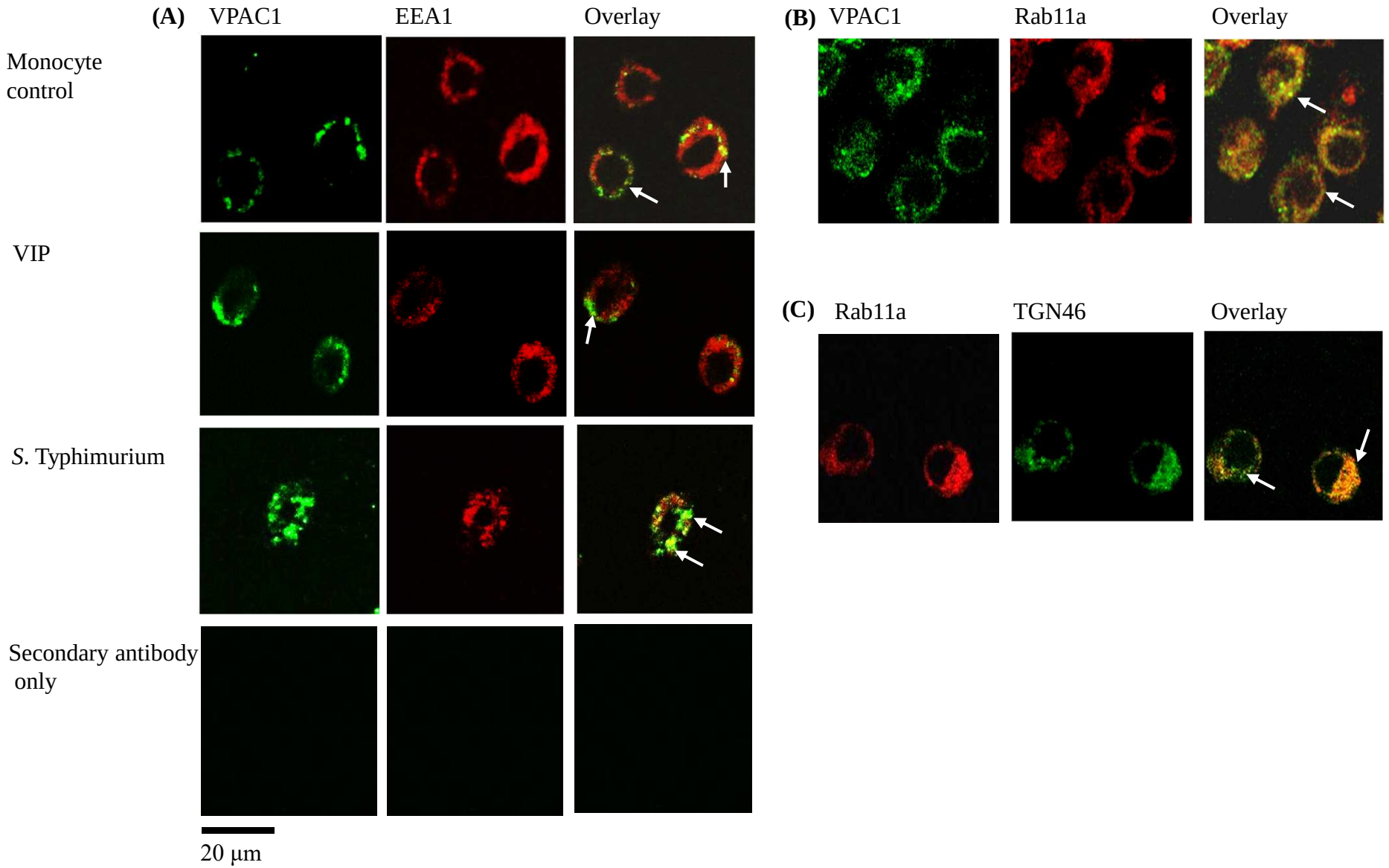


Fig 4. Askar et al

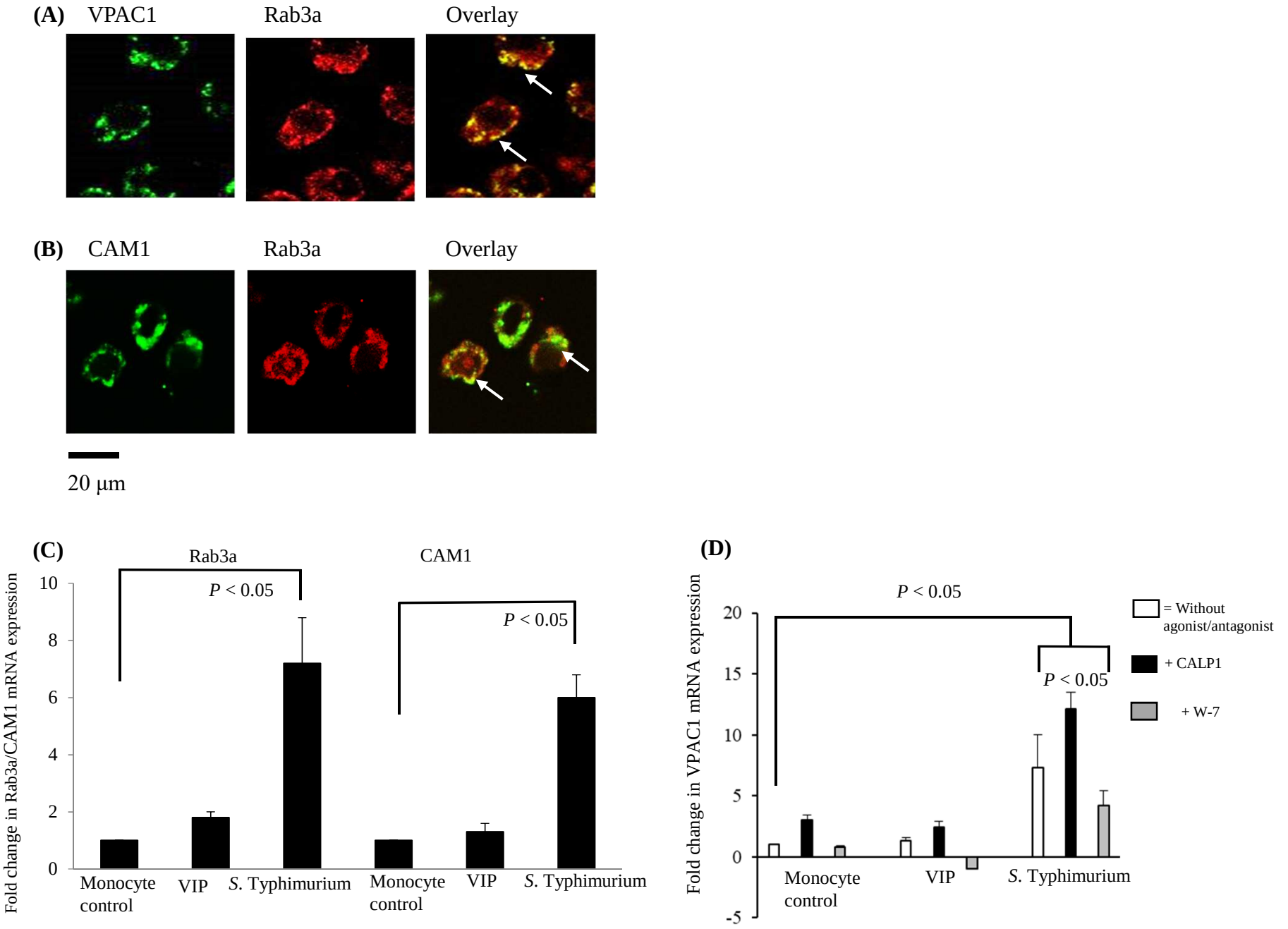


Fig 5. Askar et al

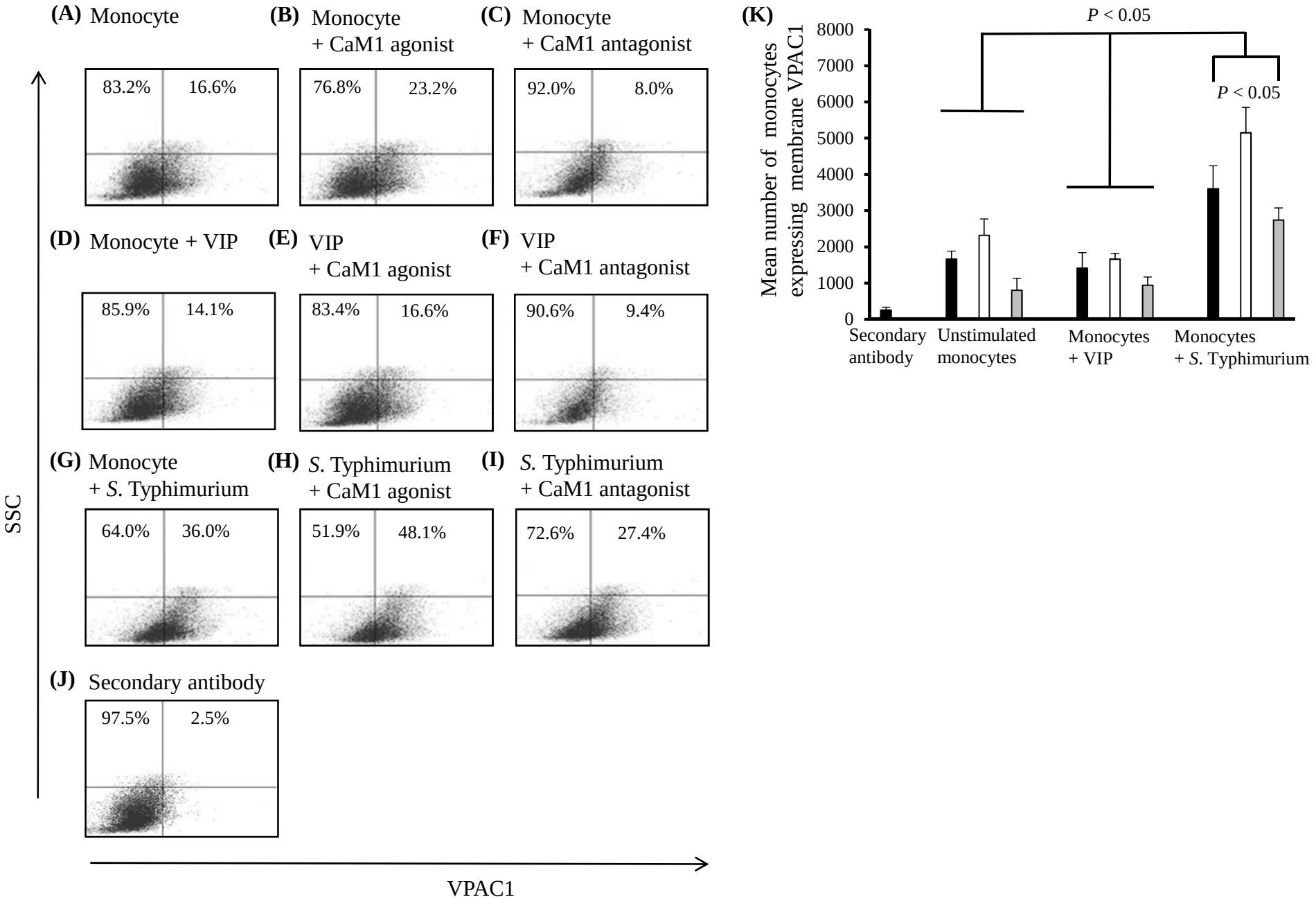


Fig 5. Askar et al

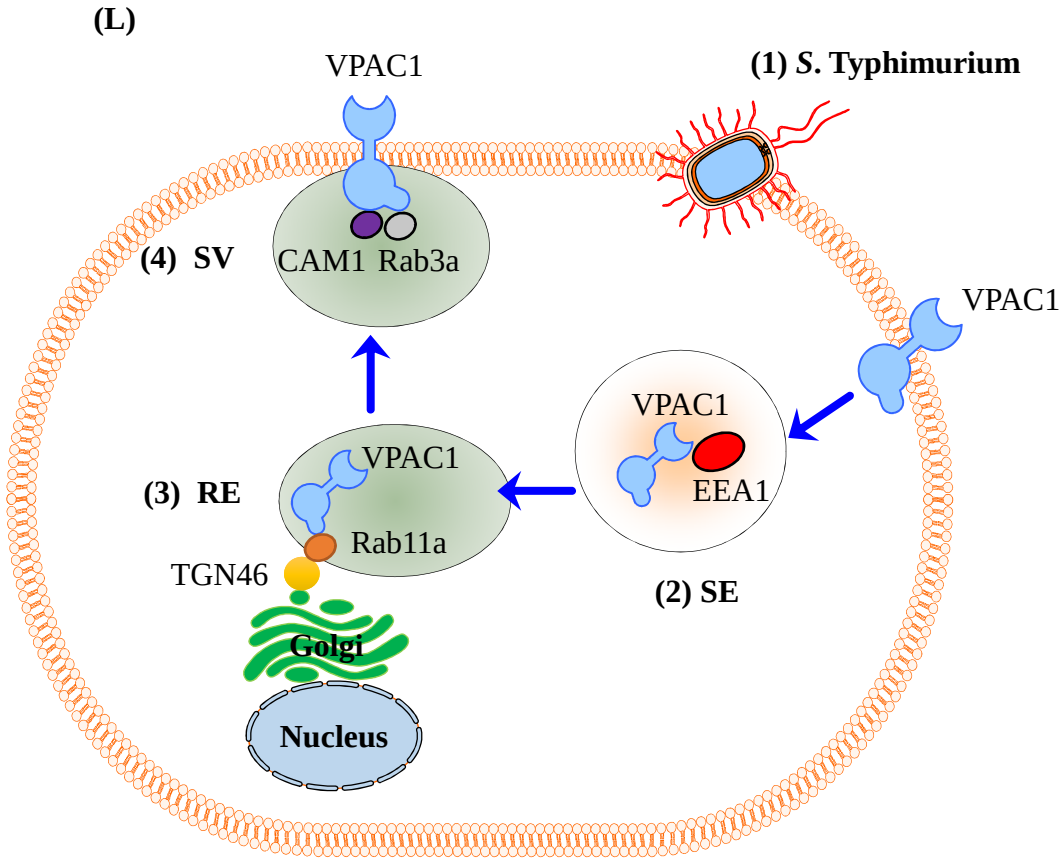


Table 1. Askar et al

Gene	**Forward primer** **(5’-3’)**	**Reverse primer** **(3’-5’)**	**Probe**
VPAC1	TCCGCCAGC CACTCTATC	GCTCGAGCC TGCACAATC	#19
Rab3a	AACGAGGAA TCCTTCAATGCA	TGGGCATTGT CCCATGAGTA	TGCAGGACTGGT CCACCCAGATCA
CAM1	TGCATTCAGGGC TGATTTATAGAG	AACAAGCTACAA AATGCCAGAAAGA	CCCTTGGCTTCTC CTTCTCCTACTCCCT
β-actin	CCAACCGCG AGAAGATGA	CCAGAGGAGT ACAGGGATAG	#64

Table 2. Askar et al

Receptor	**Primary antibody**	**Conc. (µg/ml)**	**Secondary antibody**	**Conc. (µg/ml)**
VPAC1	Mouse anti-human IgG2a (Abcam, Cambs, UK)	1	Rat anti-mouse IgG2a-Alexa 488 (Abcam, Camb, UK)	0.1
EEA1	Rabbit anti-human IgG (Abcam, Camb, UK)	1	Donkey anti-rabbit IgG-Alexa 647 (Abcam, Camb, UK)	2
Rab3a	Rabbit anti-human IgG (Abcam, Camb, UK)	1	Donkey anti-rabbit IgG-Alexa 647 647 (Abcam, Camb, UK)	2
CAM1	Mouse anti-human IgG1 (Abcam, Camb, UK)	2	Rat anti-mouse IgG1-Alexa 488 (Invitrogen, Frederick, USA)	1
Rab11a	Rabbit anti-human IgG (Abcam, Camb, UK)	1	Donkey anti-rabbit IgG Alexa 647 647 (Abcam, Camb, UK)	2
TGN46	Mouse anti-human IgG1 (Abcam, Camb, UK)	5	Rat anti-mouse IgG1-Alexa 488 (Invitrogen, Frederick, USA)	1